DEUTSCHES ELEKTRONEN-SYNCHROTRON

DESY 94-068
April 1994

Impedances in Lossy Elliptical Vacuum Chambers

A. Piwinski

Deutsches Elektronen-Synchrotron DESY, Hamburg

ISSN 0418-9833

NOTKESTRASSE 85 - 22603 HAMBURG

DESY 94-068
April 1994

ISSN 0418-9833

IMPEDANCES IN LOSSY ELLIPTICAL VACUUM CHAMBERS

A. Piwinski

Abstract
The wake fields of a bunched beam caused by the resistivity of the chamber walls are investigated for a vacuum chamber with elliptical cross section. The longitudinal and transverse impedances are calculated for arbitrary energies and for an arbitrary position of the beam in the chamber.

1. Introduction

With increasing length of accelerators the vacuum chambers became smaller and the impedances due to the resistivity of the chamber walls became larger. On the other hand, the number of discontinuities in the chamber, such as bellows, was reduced by more sophisticated design so that the contribution of the lossy smooth chamber to the total impedances became more significant. In linear colliders with very narrow vacuum chambers the resistive impedances are also important.

The wake fields of a bunched beam with relativistic energy caused by the resistivity of the vacuum chamber walls have been studied in detail for round vacuum chambers [2, 3, 11] and for flat chambers, represented by two infinite parallel plates [5, 7, 10]. As a particular result of these investigations it turned out that the longitudinal impedance and the ohmic losses are equal in the three cases when the beam is

(a) in the center of a round chamber,

(b) midway between two infinite parallel plates,

(c) parallel to a single infinite plate,

assuming that the radius of the round chamber equals the distance of the beam to the plates.

In the case of a round chamber it was shown that the longitudinal impedance and the losses pass a minimum when the radius of the pipe increases, while the smallest distance of the beam to the chamber wall remains constant [11], i. e. when case (a) changes to case (c) since an infinite radius means a single plate. The minimum is 83 % of the value in the limiting cases and it occurs when the radius is about 1.7 times the smallest distance of the beam to the chamber wall.

In the case of a flat chamber it was shown that the longitudinal impedance and the losses pass a minimum when the distance of the beam to one plate increases, while the distance to the other plate remains constant [10], i. e. when case (b) changes to case (c). The minimum occurs when the distance of the beam to one plate is about twice the distance to the other plate, and its value is 87 % of that in the limiting cases.

In the following analysis the wake fields of a bunched beam with an arbitrary position in an elliptical vacuum chamber are investigated. It turns out that the longitudinal impedance and the ohmic losses pass a minimum when the major radius of the elliptical chamber increases, while the minor radius remains constant, i. e. when case (a) changes to case (b). The minimum occurs when the major radius is about 1.4 times the minor radius and its value is 93% of the value of a round or a flat chamber.

According to these results the longitudinal impedance and the ohmic losses in an elliptical chamber are then only slightly smaller than in a round chamber with a radius equal to the minor radius of the elliptical chamber, but they are much larger than those determined with the usual assumption that they can be calculated by the mean value of the minor and major radius of the elliptical cross section.

The transverse impedances do not have the same properties in the limiting cases as the longitudinal impedance. They increase or decrease continuously when one limiting case changes to an other. Thus, in the center of a round chamber, the transverse impedance is slightly smaller by a factor of $8/\pi^2$ than in the middle of a flat vacuum chamber. The transverse impedances also show a different behaviour when the beam is displaced from the center of the chamber, for example due to orbit distortions. For the elliptical chamber we will discuss especially the increase of the impedances with a displacement of the beam, which is considerably larger for the transverse impedances than for the longitudinal impedance.

We will use here the same method for the calculation of the wake field forces as in Ref. [5, 10, 11] and represent the total electro-magnetic field by a superposition of field harmonics. With this method, arbitrary energies and arbitrary positions of the beam in the chamber can be considered. It is then also easy to show a reciprocity property which says that the longitudinal wake field force is unchanged when the test particle and the beam are interchanged.

2. Representation of the Electro-Magnetic Field by Field Harmonics

2.1 Field Harmonics in an Elliptical Coordinate System

The transverse rectangular coordinates x, y are transformed by

$$x = c \cosh\eta \cos\psi \tag{1}$$
$$y = c \sinh\eta \sin\psi \tag{2}$$

into elliptical coordinates η, ψ whereas the longitudinal coordinate s is unchanged. c is the eccentricity of all ellipses given by η = constant. It is determined by the cross section of the vacuum chamber [1]. The field harmonics can be represented by the vectors

$$\vec{e}_{nCc}(\eta,\psi,s) = \frac{1}{g(\eta,\psi)}\left\{ Ce_n(\eta)\, ce'_n(\psi),\ -Ce'_n(\eta)\, ce_n(\psi),\ 0\ \right\} \exp\{i(ks-\omega t)\} \tag{3}$$

with

$$g^2(\eta,\psi) = \cosh^2\eta - \cos^2\psi\,. \tag{4}$$

$k = \omega/v$ is the wave number, v is the velocity of the beam, and ω is the angular frequency of the field harmonics. $ce_n(\psi)$ is the even periodic Mathieu function and $ce'_n(\psi)$ is $dce_n(\psi)/d\psi$. $ce_n(\psi)$ can be replaced by $se_n(\psi)$, the odd periodic Mathieu function. $Ce_n(\eta)$ is the modified Mathieu function and $Ce'_n(\eta)$ is $dCe_n(\eta)/d\eta$. $Ce_n(\eta)$ can be replaced by $Se_n(\eta)$ so that Eq.(3) defines the four different vectors $\vec{e}_{nCc}$, $\vec{e}_{nCs}$, $\vec{e}_{nSc}$, and $\vec{e}_{nSs}$. The Mathieu functions satisfy the differential equations [14,16]

$$\frac{d^2 fe_n}{d\psi^2} + (p - 2q\cos(2\psi))fe_n = 0 \tag{5}$$

$$\frac{d^2 Fe_n}{d\eta^2} - (p - 2q\cosh(2\eta))Fe_n = 0 \tag{6}$$

where fe_n stands for ce_n or se_n, and Fe_n stands for $Ce_n(\eta)$ or $Se_n(\eta)$. p is an eigenvalue which is determined by the periodicity of ce_n and se_n. With [14]

$$\begin{aligned} \text{curl}\ \vec{e}_{nCc} &= \left\{ \frac{1}{cg}\frac{\partial e_s}{\partial\psi} - \frac{\partial e_\psi}{\partial s},\ \frac{\partial e_\eta}{\partial s} - \frac{1}{cg}\frac{\partial e_s}{\partial\eta},\ \frac{1}{cg^2}\left(\frac{\partial}{\partial\eta}(g\, e_\psi) - \frac{\partial}{\partial\psi}(g\, e_\eta)\right)\right\} \\ &= \left\{ \frac{ik}{g}Ce'_n ce_n,\ \frac{ik}{g}Ce_n ce'_n,\ \frac{4q}{c}Ce_n ce_n \right\} \exp\{i(ks-\omega t)\} \end{aligned} \tag{7}$$

one obtains

$$\text{curl curl}\ \vec{e}_{nCc} = (k^2 + 4q/c^2)\, \vec{e}_{nCc}\,. \tag{8}$$

Thus the vectors $\vec{e}_{nCc}$ satisfy the wave equation if q satisfies the condition

$$k^2 + 4q/c^2 = \omega^2/c_\ell^2 \quad \text{or} \quad 4q/c^2 = -k^2/\gamma^2 \tag{9}$$

with

$$\gamma = \frac{1}{\sqrt{1-\beta^2}}, \qquad \beta = \frac{v}{c_\ell}$$

c_ℓ is the velocity of light. The total field produced by the bunch is then given by

$$\{\vec{E}, \vec{B}\} = \sum_{n=0}^{\infty} \int_{-\infty}^{\infty} \{\vec{E}_n, \vec{B}_n\}\, d\omega \tag{10}$$

2.2 Representation of the Beam in an Elliptical Coordinate System

The bunched beam may be represented by a line current with Gaussian distribution in longitudinal direction. It is moving with the velocity v in the direction of s in the elliptical coordinate system $\{\eta,\psi,s\}$, and it has a horizontal displacement of $x_o = c\cosh\eta_o \cos\psi_o$ and a vertical displacement of $y_o = c\sinh\eta_o \sin\psi_o$. The space charge density ρ can then be written as

$$\rho(\eta,\psi,s,t) = \frac{eN_p}{\sqrt{2\pi}\sigma_s c^2 g^2(\eta,\psi)}\,\delta(\eta-\eta_o)\,\delta(\psi-\psi_o)\,\exp\left\{-\frac{(s-vt)^2}{2\sigma_s^2}\right\} \tag{11}$$

where e is the elementary charge, N_p is the number of particles per bunch, σ_s is the standard deviation of the longitudinal Gaussian particle distribution and δ is the Dirac function. Here it has been taken into account that the volume element $dx\,dy\,ds$ is transformed into $c^2 g^2(\eta,\psi)\, d\eta\, d\psi\, ds$. A decomposition into field harmonics for ψ and $s - vt$ gives

$$\rho(\eta,\psi,s,t) = \frac{\delta(\eta-\eta_o)}{c\, g(\eta,\psi)} \sum_{n=0}^{\infty} \int_{-\infty}^{\infty} \tilde{\lambda}_n(\psi,s,t,\omega)\, d\omega \tag{12}$$

where

$$\tilde{\lambda}_n(\psi,s,t,\omega) = \frac{\tilde{R}_n(\omega)}{c\, g(\eta_o,\psi)}\Big(ce_n(\psi)ce_n(\psi_o) + se_n(\psi)se_n(\psi_o)\Big)\exp\left\{i\omega\left(\frac{s}{v}-t\right)\right\} \tag{13}$$

is the charge density on the surface $\eta = \eta_o$ with

$$\tilde{R}_n(\omega) = \frac{eN_p}{4\pi^2 v}(2-\delta_{o,n})\exp\left\{-\frac{\omega^2\sigma_s^2}{2v^2}\right\} \tag{14}$$

and with $\delta_{o,o} = 1$, and $\delta_{o,n} = 0$ for $n \neq 0$. To represent $\delta(\psi-\psi_o)/g(\eta,\psi)$ by Mathieu functions the orthogonality properties [16]

$$\int_0^{2\pi} ce_m ce_n \, d\psi = \pi\,\delta_{m,n}(1+\delta_{o,n}) \quad (15), \qquad \int_0^{2\pi} se_m se_n \, d\psi = \pi\,\delta_{m,n}(1-\delta_{o,n}) \quad (16)$$

$$\int_0^{2\pi} ce_m se_n \, d\psi = 0 \tag{17}$$

have been used.

2.3 Chamber Walls with Infinite Conductivity

The chamber wall may be placed at $\eta = \eta_1 =$ constant. The major and minor half axis are then given by

$$a = c\cosh\eta_1 \quad (18), \qquad b = c\sinh\eta_1 \quad (19)$$

and the eccentricity c of the chamber cross section is given by

$$c^2 = a^2 - b^2 \tag{20}$$

In case of an infinite conductivity of the chamber walls, the field of the bunch can be represented in the two regions $\eta > \eta_o$ and $\eta < \eta_o$ by:

$$\pm\eta < \pm\eta_o$$

$$\begin{aligned}\tilde{\vec{E}}_n = \mathrm{curl}\Big(&A_{n1c,n2c}\,\vec{e}_{nCc,nSc} - A_{n2c}\,\vec{e}_{nCc}\,Se_n(\eta_1)/Ce_n(\eta_1)\\ &+ A_{n1s,n2s}\,\vec{e}_{nSs,nCs} - A_{n2s}\,\vec{e}_{nSs}\,Ce_n(\eta_1)/Se_n(\eta_1)\Big)\end{aligned} \tag{21}$$

$$\begin{aligned}i\omega\tilde{\vec{B}}_n = \beta^2k^2\Big(&A_{n1c,n2c}\,\vec{e}_{nCc,nSc} - A_{n2c}\,\vec{e}_{nCc}\,Se_n(\eta_1)/Ce_n(\eta_1)\\ &+ A_{n1s,n2s}\,\vec{e}_{nSs,nCs} - A_{n2s}\,\vec{e}_{nSs}\,Ce_n(\eta_1)/Se_n(\eta_1)\Big)\end{aligned} \tag{22}$$

where the vectors $\vec{e}_{nCc}$ and $\vec{e}_{nSs}$ are finite and continuous at $\eta = 0$. It is easy to see that $\tilde{E}_{n\psi}$, $\tilde{E}_{ns}$, and $\tilde{B}_{n\eta}$ vanish at $\eta = \eta_1$. The conditions of continuity for $\tilde{E}_{n\psi}$, $\tilde{E}_{ns}$ and $\tilde{B}_{n\eta}$ and the conditions for $\tilde{E}_{n\eta}$ giving the charge density $\tilde{\lambda}_n$ and for $\tilde{B}_{n\psi}$ giving the current density $v\tilde{\lambda}_n$ at $\eta = \eta_o$ yield for the four constants A_{n1c}, A_{n2c}, A_{n1s}, and A_{n2s}

$$\{A_{n1c}, A_{n2c}\} = \frac{-i\tilde{R}_n}{\epsilon_o kcK_n}\{Se_n(\eta_o), Ce_n(\eta_o)\}\,ce_n(\psi_o) \tag{23}$$

$$\{A_{n1s}, A_{n2s}\} = \frac{i\tilde{R}_n}{\epsilon_o kcK_n}\{Ce_n(\eta_o), Se_n(\eta_o)\}\,se_n(\psi_o) \tag{24}$$

with

$$K_n = Ce_n(\eta_o)Se_n'(\eta_o) - Ce_n'(\eta_o)Se_n(\eta_o) \tag{25}$$

where ϵ_o is the dielectric constant of the vacuum. K_n does not depend on η_o. This can be proven by differentiating Eq.(25) with respect to η_o and taking into account the differential equation for the Mathieu Functions (Eq.(6)).

2.4 Chamber Walls with Finite Conductivity

In order to take into account a finite but large conductivity σ of the chamber wall we set at $\eta{=}\eta_1$

$$\tilde{E}_{n\psi,ns} = \mp\frac{i\omega}{w}\tilde{B}_{ns,n\psi} \tag{26}$$

with

$$w = \sqrt{-i\omega\mu\sigma}\,, \qquad Re\{w\} \geq 0$$

where σ is the conductivity and μ is the permeability of the chamber wall. This approximation for the field of a line current moving parallel to a smooth wall is valid if the following three conditions for the skin depth d_s are satisfied [10,11]:

$$d_s \ll \mathrm{Min}\{d_{wall},\ d_{bw},\ 1/(b\,k^2)\}$$

where the skin depth is defined by

$$d_s = \sqrt{\frac{2}{|\omega|\mu\sigma}} = \frac{\sqrt{2}}{|w|} \tag{27}$$

and d_{wall} and d_{bw} are the thickness of the wall and the distance of the beam to the wall, respectively. Since d_s depends on $k = \omega/v$ the condition for the validity of Eq.(26) can also be written as

$$\mathrm{Max}\{1/(\beta\sigma Z_o d_{wall}^2),\ 1/(\beta\sigma Z_o d_{bw}^2)\} \ll k \ll (\beta\sigma Z_o/b^3)^{1/3}$$

where $Z_o = 377$ Ohm is the impedance of the vacuum. With Eq.(14) one obtains also a lower limit for the bunch length:

$$\sigma_s^3 \gg \frac{b^2}{\beta\sigma Z_o}$$

σZ_o is about 2×10^7/mm for copper, and the last condition is satisfied in all existing accelerators. A very short bunch length [8,9] is not considered here. The magnetic field components on the right side of Eq.(26) are the values in the case of infinite conductivity. For the case of finite conductivity the electric and magnetic field can then be written as

$$\pm\eta < \pm\eta_o$$

$$\begin{aligned}\tilde{\vec{E}}_n &= \mathrm{curl}\Big(A_{n1c,n2c}\,\vec{e}_{nCc,nSc} - A_{n2c}\,\vec{e}_{nCc}\,Se_n(\eta_1)/Ce_n(\eta_1)\\ &\qquad + A_{n1s,n2s}\,\vec{e}_{nSs,nCs} - A_{n2s}\,\vec{e}_{nSs}\,Ce_n(\eta_1)/Se_n(\eta_1)\Big)\\ &\quad + \frac{1}{w}\sum_{m=0}^{\infty}\Big(\mathrm{curl}\,(G_{nmc}\,\vec{e}_{mCc} + G_{nms}\,\vec{e}_{mSs}) + P_{nmc}\,\vec{e}_{mCc} + P_{nms}\,\vec{e}_{mSs}\Big) \qquad (28)\end{aligned}$$

$$\begin{aligned}i\omega\tilde{\vec{B}}_n &= \mathrm{curl}\,\tilde{\vec{E}}_n\\ &= \beta^2k^2\Big(A_{n1c,n2c}\,\vec{e}_{nCc,nSc} - A_{n2c}\,\vec{e}_{nCc}\,Se_n(\eta_1)/Ce_n(\eta_1)\\ &\qquad + A_{n1s,n2s}\,\vec{e}_{nSs,nCs} - A_{n2s}\,\vec{e}_{nSs}\,Ce_n(\eta_1)/Se_n(\eta_1)\Big) \qquad (29)\\ &\quad + \frac{1}{w}\sum_{m=o}^{\infty}\Big(\beta^2k^2(G_{nmc}\,\vec{e}_{mCc} + G_{nms}\,\vec{e}_{mSs}) + \mathrm{curl}\,(P_{nmc}\,\vec{e}_{mCc} + P_{nms}\,\vec{e}_{mSs})\Big)\end{aligned}$$

An infinite sum of $\vec{e}_{mSc}$ and $\vec{e}_{mSs}$ is necessary since $\tilde{E}_{n\psi}$ and $\tilde{E}_{ns}$ do not have the same dependence on ψ as $\tilde{B}_{ns}$ and $\tilde{B}_{n\psi}$, respectively. $G_{nmc,nms}$, which describe the wake field forces, follow with Eq.(26) and the orthogonality properties Eqs.(15), (16), and (17) to

$$G_{nmc} = \frac{\beta^2\gamma^2 A_{n2c}(2-\delta_{o,m})\,K_n}{2\pi c\,Ce_n(\eta_1)Ce_m(\eta_1)}\int_0^{2\pi}\frac{ce_n(\phi)\,ce_m(\phi)\,d\phi}{\sqrt{\cosh^2\eta_1-\cos^2\phi}} \qquad (30)$$

$$G_{nms} = -\frac{\beta^2\gamma^2 A_{n2s}K_n}{\pi c Se_n(\eta_1)Se_m(\eta_1)}\int_0^{2\pi}\frac{se_n(\phi)\,se_m(\phi)\,d\phi}{\sqrt{\cosh^2\eta_1-\cos^2\phi}} \qquad (31)$$

where K_n is defined by Eq.(25).

2.5 A Potential for the Forces caused by the Finite Conductivity

The harmonics of the longitudinal force due to the finite conductivity of the chamber wall are given by

$$\tilde{F}_{nms} = -\frac{ek^2c}{\gamma^2 w}\left(G_{nmc}Ce_m(\eta)ce_m(\psi) + G_{nms}Se_m(\eta)se_m(\psi)\right)\,\exp\{i(ks-\omega t)\} \qquad (32)$$

and the harmonics of the transverse forces are given by

$$\begin{aligned}\tilde{F}_{nm\eta} &= e\,(\tilde{E}_{nm\eta} - v\tilde{B}_{nm\psi})\\ &= \frac{ike}{\gamma^2 wg}\left(G_{nmc}Ce'_m(\eta)ce_m(\psi) + G_{nms}Se'_m(\eta)se_m(\psi)\right)\,\exp\{i(ks-\omega t)\}\end{aligned} \qquad (33)$$

and

$$\begin{aligned}\tilde{F}_{nm\psi} &= e\,(\tilde{E}_{nm\psi} + v\tilde{B}_{nm\eta})\\ &= \frac{ike}{\gamma^2 wg}\left(G_{nmc}Ce_m(\eta)ce'_m(\psi) + G_{nms}Se_m(\eta)se'_m(\psi)\right)\,\exp\{i(ks-\omega t)\}\end{aligned} \qquad (34)$$

The forces can now be written in the form

$$\begin{aligned}\{\tilde{F}_\eta,\,\tilde{F}_\psi,\,\tilde{F}_s\} &= \sum_{m=0}^{\infty}\sum_{n=0}^{\infty}\{\tilde{F}_{nm\eta},\,\tilde{F}_{nm\psi},\,\tilde{F}_{nms}\}\\ &= -\left\{\frac{1}{cg}\frac{\partial}{\partial\eta},\,\frac{1}{cg}\frac{\partial}{\partial\psi},\,\frac{\partial}{\partial s}\right\}\tilde{\Phi}\end{aligned} \qquad (35)$$

where the potential $\tilde{\Phi}$ is given by

$$\begin{aligned}\tilde{\Phi} &= -\frac{iekc}{\gamma^2 w}\sum_{n=0}^{\infty}\sum_{m=0}^{\infty}\left(G_{nmc}Ce_m(\eta)ce_m(\psi) + G_{nms}Se_m(\eta)se_m(\psi)\right)\,\exp\{i(ks-\omega t)\}\\ &= -\frac{\beta^2 r_e E_o N_p}{2\pi^2 vbw}\,H(\eta,\psi,\eta_o,\psi_o)\,\exp\left\{-\frac{\omega^2\sigma_s^2}{2v^2} + i(ks-\omega t)\right\}\end{aligned} \qquad (36)$$

The function $H(\eta,\psi,\eta_o,\psi_o)$ is defined by

$$H(\eta,\psi,\eta_o,\psi_o) = \frac{1}{2\pi}\int_0^{2\pi}\frac{f_c(\eta,\psi,\phi)f_c(\eta_o,\psi_o,\phi) + f_s(\eta,\psi,\phi)f_s(\eta_o,\psi_o,\phi)}{\sqrt{1+\sin^2\phi/\sinh^2\eta_1}}\,d\phi \qquad (37)$$

with $\cosh^2\eta_1 - \cos^2\phi = \sinh^2\eta_1 + \sin^2\phi$, and

$$f_c(\eta,\psi,\phi) = \sum_{m=0}^{\infty}(2-\delta_{o,m})\frac{Ce_m(\eta)}{Ce_m(\eta_1)}\,ce_m(\psi)\,ce_m(\phi) \qquad (38)$$

$$f_s(\eta,\psi,\phi) = 2\sum_{m=0}^{\infty}\frac{Se_m(\eta)}{Se_m(\eta_1)}\,se_m(\psi)\,se_m(\phi) \qquad (39)$$

Integration of Eq.(36) with respect to ω gives [2, 10, 11]

$$\Phi = -\frac{\beta r_e E_o N_p}{b\sqrt{2\mu_r Z_o\sigma}}\,H(\eta,\psi,\eta_o,\psi_o)\left|\frac{\beta u}{\sigma_s}\right|^{1/2}\left(I_{-1/4}\mp I_{1/4}\right)e^{-u^2/4} \qquad (40)$$

for $\pm(s-vt)\geq 0$. The argument of the Bessel functions I_ν is $u^2/4$, where u is defined by

$$u = \frac{s-vt}{\sigma_s}$$

and the total forces can be written as

$$\{F_\eta,\,F_\psi,\,F_s\} = -\left\{\frac{1}{cg}\frac{\partial}{\partial\eta},\,\frac{1}{cg}\frac{\partial}{\partial\psi},\,\frac{\partial}{\partial s}\right\}\Phi \qquad (41)$$

Eqs.(37) and (40) show that the potential Φ is unchanged when η and ψ are interchanged with η_o and ψ_o, as in the case of Greens functions. This means in particular that the longitudinal force F_s is unchanged when a test particle at the position $\{\eta,\psi\}$ is interchanged with the beam at the position $\{\eta_o,\psi_o\}$.

2.6 Approximations of the Mathieu Functions for large γ

There is no principle difficulty in calculating the wake field forces and the impedances with the function $H(\eta,\psi,\eta_o,\psi_o)$ as defined by Eqs.(37), (38), and (39) for arbitrary beam energies. The Mathieu Functions can be evaluated by series expansion in trigonometric and hyperbolic functions [16]. But for most practical problems the energies are large and we will derive approximations for relativistic energies which simplify the results and reduce the computer time.

If the terms with q in Eqs.(5) and (6) may be neglected against p the Mathieu functions are approximately given by

$$ce_n(\psi) = \cos(n\psi) \quad (42), \qquad se_n(\psi) = \sin(n\psi) \quad (43)$$

$$Ce_n(\eta) = \cosh(n\eta) \quad (44), \qquad Se_n(\eta) = \sinh(n\eta) \quad (45)$$

With $p = n^2$ and with $2q\cosh(2\eta) \le 2q\cosh(2\eta_1) = 8k^2(a^2+b^2)/\gamma^2$ one obtains for this approximation the condition

$$\gamma^2 \gg 8k^2(a^2+b^2)/n^2$$

The largest k is of the order $1/\sigma_s$, and n runs from 1 to about $1/\eta_1 = 2/\ln((a+b)/(a-b))$. If a is large compared to b, η_1 is approximately b/a and the conditions for γ can be written as

$$\gamma^2 \gg \mathrm{Max}\{\,1,\ b^2/\sigma_s^2\,\}$$

The functions f_c and f_s take the form

$$f_c(\eta,\psi,\phi) = 1 + 2\sum_{m=1}^{\infty}\frac{\cosh(m\eta)}{\cosh(m\eta_1)}\cos(m\psi)\cos(m\phi) \qquad (46)$$

$$f_s(\eta,\psi,\phi) = 2\sum_{m=1}^{\infty}\frac{\sinh(m\eta)}{\sinh(m\eta_1)}\sin(m\psi)\sin(m\phi) \qquad (47)$$

For a numerical evaluation of the function $H(\eta,\eta_o,\psi,\psi_o)$ see App.1.

3. Wake Field Forces

3.1 Longitudinal Wake Field Force

The harmonics of the longitudinal force due to the finite conductivity of the chamber wall follow from Eqs.(35) and (36) to

$$\tilde{F}_s = \frac{i\omega\beta^2 r_e E_o N_p}{\pi v^2 b w} H(\eta,\psi,\eta_o,\psi_o)\exp\Big\{-\frac{\omega^2\sigma_s^2}{2v^2} - i(ks-\omega t)\Big\} \qquad (48)$$

and the total longitudinal force is given by (Eqs.(40) and (41))

$$F_s = \frac{r_e E_o N_p}{2b\sqrt{2\mu_r Z_o\sigma}} H(\eta,\psi,\eta_o,\psi_o)\left|\frac{\beta u}{\sigma_s}\right|^{3/2}\Big(I_{1/4} - I_{-3/4} \pm I_{3/4} \mp I_{-1/4}\Big)e^{-u^2/4} \qquad (49)$$

for $\pm(s-vt) \ge 0$. The longitudinal distribution of the longitudinal wake field force is independent of the transverse coordinates. It is plotted in Fig. 1 as a function of $s-vt$. The calculation is done for relativistic energy as in all other figures. Fig. 2 shows the dependence of the longitudinal force at the position of the beam on the ratio a/b for different vertical displacements of the beam. Figs. 3 and 4 show the longitudinal force as a function of horizontal and vertical displacements of the beam for different ratios a/b. The curve for zero displacement in Fig. 2 was also obtained in Ref.[13] with a different method using a numerical approximation for Maxwell's equations. An approximation method which was proposed in Ref. [6] has not yet been carried out.

In the limiting case of a round chamber with a radius r_1 one gets for relativistic energies with $\eta_1 \to \infty$ and $c \to 0$ but $c\cosh\eta_1 = c\sinh\eta_1 = r_1$, $c\cosh\eta_o = c\sinh\eta_o = r_o$, and $c\cosh\eta = c\sinh\eta = r$ [11]:

$$H_r(r,r_o,\psi) = \frac{r_1^4 - r^2 r_o^2}{r_1^4 - 2r_1^2 r r_o\cos\psi + r^2 r_o^2} \qquad (50)$$

and

$$F_s = \frac{r_e E_o N_p}{2r_1\sqrt{2\mu_r Z_o\sigma}}\,\frac{r_1^4 - r^2 r_o^2}{r_1^4 - 2r_1^2 r r_o\cos\psi + r^2 r_o^2}\left|\frac{u}{\sigma_s}\right|^{3/2}\Big(I_{1/4} - I_{-3/4} \pm I_{3/4} \mp I_{-1/4}\Big)e^{-u^2/4} \qquad (51)$$

where ψ is now the angle between the radii of the beam and the test particle. In the limiting case of a flat chamber with a total height of h one gets for relativistic energies with $\eta_1 \to 0$ and $c \to \infty$ but $c\sinh\eta_1 = b = h/2$ [10]:

$$H_f(x,y,y_o) = \frac{\pi}{2h}\left(\frac{-x\sinh(\pi x/h) + (y+y_o)\sin(\pi(y+y_o)/h)}{\cosh(\pi x/h) + \cos(\pi(y+y_o)/h)} + \frac{x\sinh(\pi x/h) + (y-y_o)\sin(\pi(y-y_o)/h)}{\cosh(\pi x/h) - \cos(\pi(y-y_o)/h)}\right) \qquad (52)$$

and

$$F_s = \frac{r_e E_o N_p}{h\sqrt{2\mu_r Z_o\sigma}} H_f(x,y,y_o)\left|\frac{u}{\sigma_s}\right|^{3/2}\Big(I_{1/4} - I_{-3/4} \pm I_{3/4} \mp I_{-1/4}\Big)e^{-u^2/4} \qquad (53)$$

3.2 Transverse Wake Field Forces

The harmonics of the transverse forces caused by the finite conductivity of the chamber walls are given by Eqs.(33), (34) and (35) in terms of unit vectors in the elliptical coordinate system. With $\vec{e}_{\eta,\psi} = (\sinh\eta\cos\psi\,\vec{e}_{x,y} \pm \cosh\eta\sin\psi\,\vec{e}_{y,x})/g$, where

$\vec{e}_{x,y}$ are the unit vectors in the rectangular coordinate system, one obtains for the horizontal and vertical forces

$$\tilde{F}_x = -\frac{1}{cg^2}\Big(\sinh\eta\cos\psi\frac{\partial\tilde{\Phi}}{\partial\eta} - \cosh\eta\sin\psi\frac{\partial\tilde{\Phi}}{\partial\psi}\Big) \tag{54}$$

$$\tilde{F}_y = -\frac{1}{cg^2}\Big(\cosh\eta\sin\psi\frac{\partial\tilde{\Phi}}{\partial\eta} + \sinh\eta\cos\psi\frac{\partial\tilde{\Phi}}{\partial\psi}\Big) \tag{55}$$

and the total transverse forces are given by

$$F_x = \frac{\beta r_e E_o N_p\sqrt{\beta|u|}}{bc\sqrt{2\mu_r Z_o\sigma\sigma_s}g^2}\Big(\sinh\eta\cos\psi\frac{\partial H}{\partial\eta} - \cosh\eta\sin\psi\frac{\partial H}{\partial\psi}\Big)\Big(I_{-1/4}\mp I_{1/4}\Big)\,e^{-u^2/4} \tag{56}$$

$$F_y = \frac{\beta r_e E_o N_p\sqrt{\beta|u|}}{bc\sqrt{2\mu_r Z_o\sigma\sigma_s}g^2}\Big(\cosh\eta\sin\psi\frac{\partial H}{\partial\eta} + \sinh\eta\cos\psi\frac{\partial H}{\partial\psi}\Big)\Big(I_{-1/4}\mp I_{1/4}\Big)\,e^{-u^2/4} \tag{57}$$

The longitudinal distribution is the same for the horizontal and vertical wake field forces and does not depend on the transverse position of the beam. It is plotted in Fig. 1 as a function of $s-vt$ for arbitrary x_o and y_o but $x_o^2+y_o^2\neq 0$. Figs. 5 and 6 show the dependence of the horizontal and vertical forces on the horizontal and vertical position of the beam for different ratios a/b, respectively.

In the limiting case of a round chamber one gets for relativistic energies [11]

$$\{F_r,\,F_\psi\} = \frac{2r_e E_o N_p r_o r_1\sqrt{|u|}}{\sqrt{2\mu_r Z_o\sigma\sigma_s}}\,\frac{\{(r_1^4+r_o^2r^2)\cos\psi - 2r_1^2r_or,\;\; 2r_1(r_o^2r^2-r_1^4)\sin\psi\}}{(r_1^4-2r_1^2r_or\cos\psi+r_o^2r^2)^2} \times\big(I_{-1/4}\mp I_{1/4}\big)\,e^{-u^2/4} \tag{58}$$

which simplifies for the force acting on the beam ($r=r_0$, $\psi=0$) to

$$F_r = \frac{2r_e E_o N_p\sqrt{|u|}}{\sqrt{2\mu_r Z_o\sigma\sigma_s}}\,\frac{r_o r_1}{(r_1^2-r_o^2)^2}\,\big(I_{-1/4}\mp I_{1/4}\big)\,e^{-u^2/4} \tag{59}$$

In the limiting case of a flat chamber one obtains [10]

$$\{F_x,\,F_y\} = \frac{2\pi^2 r_e E_o N_p\sqrt{|u|}}{h^2\sqrt{2\mu_r Z_o\sigma\sigma_s}}\left\{\frac{\partial H_f}{\partial x},\,\frac{\partial H_f}{\partial y}\right\}\Big(I_{-1/4}\mp I_{1/4}\Big)\,e^{-u^2/4} \tag{60}$$

where H_f is given by Eq.(52). For the force on the beam ($x=0$, $y=y_o$) one obtains

$$F_y = \frac{\pi^3 r_e E_o N_p\sqrt{|u|}}{2h^3\sqrt{2\mu_r Z_o\sigma\sigma_s}}\,\frac{2\pi y_o/h+\sin(2\pi y_o/h)}{\cos^2(\pi y_o/h)}\Big(I_{-1/4}\mp I_{1/4}\Big)\,e^{-u^2/4}$$

4. Impedances

4.1 Longitudinal Impedance

The longitudinal impedance per unit length can be defined by [4]

$$Z_\ell' = -\frac{\tilde{U}_\ell}{L\tilde{I}} \tag{61}$$

with

$$\frac{\tilde{U}_\ell}{L} = \sum_{n=0}^{\infty}\sum_{m=0}^{\infty}\tilde{E}_{nms}\,\exp\{-i(ks-\omega t)\} = \frac{(i\mp 1)\beta^2\omega\tilde{R}_o}{\epsilon_o vb\sqrt{2|\omega|\mu\sigma}}\,H(\eta_o,\psi_o,\eta_o,\psi_o) \tag{62}$$

for $\pm\omega>0$, where the field has to be taken at $\eta=\eta_o$ and $\psi=\psi_o$. The harmonics of the current are given by

$$\tilde{I}(\omega) = v\int\!\!\int\tilde{\rho}\,dx\,dy\,\exp\{-i(ks-\omega t)\} = 2\pi v\tilde{R}_o(\omega) \tag{63}$$

since

$$I(s,t) = \frac{veN_p}{\sqrt{2\pi}\sigma_s}\exp\Big\{-\frac{(s-vt)}{2\sigma_s^2}\Big\} = \int_{-\infty}^{\infty}\tilde{I}(\omega)\,\exp\{i(ks-\omega t)\}\,d\omega$$

The longitudinal impedance can then be written in the form

$$Z_\ell' = \frac{1\mp i}{2\pi b}\sqrt{\frac{\mu_o|\omega|}{2\mu_r\sigma}}\,H(\eta_o,\psi_o,\eta_o,\psi_o) \tag{64}$$

Figs. 2, 3, and 4 show the longitudinal impedance in a normalized representation which is identical with the normalized longitudinal force. The lower curve for zero displacement in Fig. 2 approaches 1 for large a/b, i. e. the longitudinal impedance is the same in a round chamber ($a/b=1$) and in a flat chamber ($a/b\to\infty$), and it has at $a/b=1.4038$ a minimum of 92.860% of the value in a round or flat chamber.

In the special case where the beam is in the center of the elliptical chamber the longitudinal impedance simplifies to an expression which was already obtained in Ref.[12]:

$$Z_\ell' = \frac{1\mp i}{4\pi^2 b}\sqrt{\frac{\mu_o|\omega|}{2\mu_r\sigma}}\sum_{n=0}^{\infty}\sum_{m=0}^{\infty}\frac{(-1)^{n+m}(2-\delta_{o,n})(2-\delta_{o,m})}{\cosh(n\eta_1)\cosh(m\eta_1)}\int_0^{2\pi}\frac{\cos(n\phi)\cos(m\phi)}{\sqrt{1+\sin^2\phi/\sinh^2\eta_1}}\,d\phi \tag{65}$$

In the case of a round chamber ($\eta_1 \to \infty, c \to 0$, etc.) and for relativistic energies the longitudinal impedance takes the form [11]

$$Z'_{\ell r} = \frac{1 \mp i}{2\pi r_1}\sqrt{\frac{|\omega|\mu}{2\sigma}}\,\frac{r_1^2 + r_o^2}{r_1^2 - r_o^2} \tag{66}$$

where r_1 is the radius of the chamber and r_o is the position of the beam. Eq.(66) shows that the longitudinal impedance is the same in the two cases where the beam is in the center of the chamber ($r_o = 0$) or where the beam is parallel to an infinite plate ($r_o \to \infty, r_1 \to \infty, r_1 - r_o =$ const.) with a distance $r_1 - r_o$ equal to the chamber radius of the first case. The minimum of the longitudinal impedance as a function of the chamber radius r_1 for constant distance of the beam to the chamber wall is $2(\sqrt{2}-1) = 0.8284$ of the maximum, and it occurs at $r_1/(r_1 - r_o) = 1/(2-\sqrt{2}) = 1.707$.

In the case of a flat chamber ($\eta_1 \to 0, c \to \infty$, etc.) and for relativistic energies the longitudinal impedance takes the form [10]

$$Z'_{\ell f} = \frac{1 \mp i}{\pi h}\sqrt{\frac{|\omega|\mu}{2\sigma}}\left(1 + \frac{\pi y_o}{h}\tan\left(\frac{\pi y_o}{h}\right)\right) \tag{67}$$

where h is the distance between the two parallel plates and y_o is the position of the beam. Eq.(67) shows that the longitudinal impedance is the same in the two cases where the beam is midway between two parallel infinite plates ($y_o = 0$) or where one plate is removed ($y_o \to \infty, h \to \infty$, $h/2 - y_o =$const.). The minimum can be found by differentiating Eq.(67) with respect to h with $y_o = h/2 - h_o/2$ where h_o is the distance between the plates for $y_o = 0$. A numerical evaluation gives a minimum of 0.8679 times the impedance of the symmetric case, and it occurs at a distance which is $h/2 - y_o = 1.917$ times the distance in the symmetric case.

4.2 Transverse Impedances

The horizontal impedance per unit length can be defined by [4]

$$Z'_x = \frac{1}{i}\frac{1}{L\tilde{I}}\frac{\partial \tilde{U}_x}{\partial x_o} \tag{68}$$

with

$$\begin{aligned}\frac{1}{L}\frac{\partial \tilde{U}_x}{\partial x_o} &= \frac{1}{e}\frac{\partial}{\partial x_o}\tilde{F}_x\Big|_{x=x_o}\exp\{-i(ks-\omega t)\} \\ &= \frac{\beta^2 \tilde{R}_o}{\epsilon_o b w c^2}\left(\frac{\sinh\eta_o\cos\psi_o}{g_o^2}\frac{\partial}{\partial\eta_o} - \frac{\cosh\eta_o\sin\psi_o}{g_o^2}\frac{\partial}{\partial\psi_o}\right) \\ &\quad\times\left(\frac{\sinh\eta_o\cos\psi_o}{g_o^2}\frac{\partial H}{\partial\eta}\Big|_{\substack{\eta=\eta_o\\ \psi=\psi_o}} - \frac{\cosh\eta_o\sin\psi_o}{g_o^2}\frac{\partial H}{\partial\psi}\Big|_{\substack{\eta=\eta_o\\ \psi=\psi_o}}\right)\end{aligned} \tag{69}$$

where g_o stands for $g(\eta_o, \psi_o)$. With Eq.(63) one obtains

$$\begin{aligned}Z'_x &= \frac{(\pm 1 - i)\beta}{4\pi bc^2\sqrt{2|\omega|\epsilon_o\sigma}}\left(\frac{\sinh\eta_o\cos\psi_o}{g_o^2}\frac{\partial}{\partial\eta_o} - \frac{\cosh\eta_o\sin\psi_o}{g_o^2}\frac{\partial}{\partial\psi_o}\right) \\ &\quad\times\left(\frac{\sinh\eta_o\cos\psi_o}{g_o^2}\frac{\partial H_o}{\partial\eta_o} - \frac{\cosh\eta_o\sin\psi_o}{g_o^2}\frac{\partial H_o}{\partial\psi_o}\right)\end{aligned} \tag{70}$$

since $\partial H_o/\partial\eta_o = 2\partial H/\partial\eta|_{\eta=\eta_o}$ and $\partial H_o/\partial\psi_o = 2\partial H/\partial\psi|_{\psi=\psi_o}$, where H_o stands for $H(\eta_o, \psi_o, \eta_o, \psi_o)$. The horizontal impedance is plotted in Figs. 7, 8, and 9 as a function of x_o, y_o and a/b, respectively.

When the beam is in the center of the elliptical chamber ($\eta_o = 0$, $\psi_o = \pi/2$) the horizontal impedance simplifies for relativistic energies to

$$Z'_x = \frac{\pm 1 - i}{\pi^2 bc^2\sqrt{2|\omega|\epsilon_o\sigma}}\sum_{n=1}^{\infty}\sum_{m=1}^{\infty}\frac{n\,m\,\sin(n\pi/2)\sin(m\pi/2)}{\cosh(n\eta_1)\cosh(m\eta_1)}\int_0^{2\pi}\frac{\cos(n\phi)\cos(m\phi)}{\sqrt{1+\sin^2\phi/\sinh^2\eta_1}}d\phi \tag{71}$$

For the vertical impedance one obtains in a similar way

$$\begin{aligned}Z'_y &= \frac{(\pm 1 - i)\beta}{4\pi bc^2\sqrt{2|\omega|\epsilon_o\sigma}}\left(\frac{\cosh\eta_o\sin\psi_o}{g_o^2}\frac{\partial}{\partial\eta_o} + \frac{\sinh\eta_o\cos\psi_o}{g_o^2}\frac{\partial}{\partial\psi_o}\right) \\ &\quad\times\left(\frac{\cosh\eta_o\sin\psi_o}{g_o^2}\frac{\partial H_o}{\partial\eta_o} + \frac{\sinh\eta_o\cos\psi_o}{g_o^2}\frac{\partial H_o}{\partial\psi_o}\right)\end{aligned} \tag{72}$$

The vertical impedance is plotted in Figs. 10, 11, and 12 as a function of a/b, x_o and y_o, respectively. When the beam is in the center of the elliptical chamber the vertical impedance simplifies for relativistic energies to

$$Z'_y = \frac{\pm 1 - i}{\pi^2 bc^2\sqrt{2|\omega|\epsilon_o\sigma}}\sum_{n=1}^{\infty}\sum_{m=1}^{\infty}\frac{n\,m\,\sin(n\pi/2)\sin(m\pi/2)}{\sinh(n\eta_1)\sinh(m\eta_1)}\int_0^{2\pi}\frac{\sin(n\phi)\sin(m\phi)}{\sqrt{1+\sin^2\phi/\sinh^2\eta_1}}d\phi \tag{73}$$

The expressions for Z'_x and Z'_y in the special case of a beam with relativistic energy in the center of an elliptical chamber were also obtained in Ref.[12].

In the case of a round chamber one gets, for relativistic energies [11]

$$\{Z'_{xr},\ Z'_{yr}\} = \frac{\pm 1 - i}{\pi\sqrt{2|\omega|\epsilon_o\sigma}}\,\frac{r_1\{r_1^2 + 3x_o^2 - y_o^2,\ r_1^2 + 3y_o^2 - x_o^2\}}{(r_1^2 - r_o^2)^3} \tag{74}$$

and the ratio of the longitudinal impedance to the transverse impedance, i. e. to the horizontal impedance with $y_o = 0$ or to the vertical impedance with $x_o = 0$, is

$$\frac{Z'_{\ell r}}{Z'_{tr}} = \frac{\omega}{c_\ell}\,\frac{(r_1^2 + r_o^2)(r_1^2 - r_o^2)^2}{2r_1^2\,(r_1^2 + 3r_o^2)} \tag{75}$$

In the case of a flat chamber one gets, for relativistic energies [10]

$$Z'_{tf} = \frac{\pi(\pm 1 - i)}{h^3\sqrt{2|\omega|\epsilon_o\sigma}}\,\frac{1 + (\pi y_o/h)\tan(\pi y_o/h)}{\cos^2(\pi y_o/h)} \tag{76}$$

and the ratio of the longitudinal impedance to the transverse impedance is

$$\frac{Z'_{\ell f}}{Z'_{tf}} = \frac{\omega}{c_\ell}\frac{h^2}{\pi^2}\sin^2\Big(\frac{\pi(h-2y_o)}{2h}\Big) \tag{77}$$

Eqs.(74) and (76) show that the transverse impedances increase with one over the third power of the chamber dimensions ($1/r_1^3$ or $1/d^3$) whereas, according to Eqs.(66) and (67), the longitudinal impedance increases only with one over the first power of the chamber dimensions. It is easy to see that the transverse and longitudinal impedances show the same dependence when the beam approaches the chamber wall for constant chamber dimensions, i. e. the transverse impedances increase with $1/(r_1-r_o)^3$ or $1/(d/2-y_o)^3$. For a displacement of the beam from the center of the chamber the impedances show a similar behaviour which can be seen from the figures 4 and 16. Thus a vertical displacement of the orbit from the center by 10% of the total aperture increases the vertical impedance by 22 to 27%, depending on the eccentricity of the chamber cross section, whereas the longitudinal impedance increases only by 8 to 10%. A displacement of 25% of the total aperture gives an increase of 257 to 315% for the vertical impedance and only 67 to 79% for the longitudinal impedance.

5. Examples

5.1 Ohmic Losses

The total ohmic losses due to the resistivity of the chamber wall can be calculated by

$$P_w = -v\int \rho\, E_s\, dV \tag{78}$$

where the integration has to be performed over the whole space charge of the beam. ρ and E_s are given by Eqs.(11) and (41), respectively, and one obtains with $dV = c^2g^2(\eta,\psi)\,d\eta\,d\psi\,ds$

$$\begin{aligned} P_w(x_o,y_o) &= \frac{r_e E_o N_p^2 v}{4b\sigma_s^{3/2}\sqrt{\pi Z_o\mu_r\sigma}} H(\eta_o,\psi_o,\eta_o,\psi_o)\int_{-\infty}^{\infty}(I_{-3/4}-I_{1/4})\exp\Big\{-\frac{3u^2}{4}\Big\}|u|^{3/2}du \\ &= \frac{\Gamma(3/4) r_e E_o N_p^2 v}{\pi b\sigma_s^{3/2}\sqrt{2Z_o\mu_r\sigma}} H(\eta_o,\psi_o,\eta_o,\psi_o) \end{aligned} \tag{79}$$

The last integration is solved in [10,11] and Γ is the gamma function ($\Gamma(3/4) = 1.2254...$). The ohmic losses can also be calculated by integrating the longitudinal impedance in the frequency domain [2] with Eqs.(13) and (48).

In the case of a round chamber one obtains for relativistic energies [11]

$$P_w = \frac{\Gamma(3/4) r_e E_o N_p^2 c_\ell}{\pi r_1\sigma_s^{3/2}\sqrt{2Z_o\mu_r\sigma}}\frac{r_1^2+r_o^2}{r_1^2-r_o^2} \tag{80}$$

and in the case of a flat vacuum chamber one obtains, for relativistic energies [10]:

$$P_w = \frac{2\Gamma(3/4) r_e E_o N_p^2 c_\ell}{\pi h\sigma_s^{3/2}\sqrt{2\mu_r Z_o\sigma}}\Big(1+\frac{\pi y_o}{h}\tan\Big(\frac{\pi y_o}{h}\Big)\Big) \tag{81}$$

5.2 Coherent Betatron Frequency Shift

The transverse wake field forces which vary with the transverse displacement of the beam in the chamber cause a shift of the cohefent betatron frequency but no shift of the incoherent betatron frequency. In first approximation the forces vary linearly with the displacement of the beam and the derivative of the transverse forces with respect to the beam position (Eqs.(56) and (57)) determines the tune shift. One has to average the forces over the whole longitudinal particle distribution and over the whole circumference. The tune shift is then given by

$$\Delta Q_{x,y} = -\frac{1}{4\pi}\oint \beta_{x,y}K_{x,y}\,d\ell \tag{82}$$

where $\beta_{x,y}$ are the horizontal and vertical amplitude function, respectively, and $K_{x,y}$ is, for relativistic energies, given by

$$\{K_x,\ K_y\} = \frac{1}{\sqrt{2\pi}\sigma_s E}\int_{-\infty}^{\infty}\Big\{\frac{\partial F_x}{\partial x_o},\ \frac{\partial F_y}{\partial y_o}\Big\}\exp\Big\{-\frac{(s-\omega t)^2}{2\sigma_s^2}\Big\}\,ds \tag{83}$$

where F_{xo} and F_{yo} stand for $F_x|_{x=x_o}$ and $F_y|_{y=y_o}$, respectively. With

$$\begin{aligned} \frac{\partial F_{xo}}{\partial x_o} &= \int_{-\infty}^{\infty}\frac{\partial \tilde{F}_{xo}}{\partial x_o}\,d\omega \\ &= e^2N_p(\sqrt{|\omega|}|Z'_x|)\sqrt{\frac{|u|c_\ell}{8\sigma_s}}\,I_{-1/4}(u^2/4)e^{-u^2/4} \end{aligned} \tag{84}$$

one obtains

$$K_x = \frac{2\,\Gamma(1/4) r_e N_p}{\gamma\sqrt{2c_\ell\sigma_s}}\frac{(\sqrt{|\omega|}|Z'_x|)}{Z_o} \tag{85}$$

with $\Gamma(1/4) = 3.6256...$ The integral is solved in [10,11], and the expressions for the transverse impedances (Gl.(70) and (72)) have been used, where $\sqrt{|\omega|}|Z'_x|$ is independent on ω. The tune shifts can then be written in the form:

$$\Delta Q_{x,y} = -\frac{\Gamma(1/4) r_e N_p C}{2\pi\gamma\sqrt{2c_\ell\sigma_s}\,Z_o}\Big\langle\beta_{x,y}\,(\sqrt{|\omega|}|Z'_{x,y}|)\Big\rangle \tag{86}$$

where C is the length of the circumference and the brackets denote the average over the whole circumference.

In the case of a round chamber one obtains

$$\{\Delta Q_{xr},\ \Delta Q_{yr}\} = -\frac{\Gamma(1/4)\, r_e N_p C}{2\pi^2\gamma\sqrt{2\mu_r Z_o \sigma\sigma_s}} \left\langle \frac{\{\beta_x r_1(r_1^2+3x_o^2-y_o^2),\ \beta_y r_1(r_1^2+3y_o^2-x_o^2)\}}{(r_1^2-r_o^2)^3} \right\rangle \tag{87}$$

and in the case of a flat chamber one obtains

$$\Delta Q_{yf} = -\frac{\Gamma(1/4)\, r_e N_p C}{2\gamma\sqrt{2\mu_r Z_o \sigma\sigma_s}} \left\langle \beta_y \frac{1+(\pi y_o/h)\tan(\pi y_o/h)}{h^3\cos^2(\pi y_o/h)} \right\rangle \tag{88}$$

References

[1] Lan Jen Chu, Journal of Applied Physics, Vol. 9(1938)

[2] A. Piwinski, DESY 72/72 (1972)

[3] A. Piwinski, IEEE Trans. on Nuclear Science, Vol. NS-24, No.3 (1977)

[4] A. W. Chao, SLAC-PUB-2946, 1982

[5] A. Piwinski, DESY 84-097, October1984

[6] L. Palumbo, V. G. Vaccaro, Il Nuovo Cimento, 1985, Vol. 89A, N.3, p. 243

[7] H. Henke, O. Napoly, Proc. 2nd Europ. Acc. Conf., Nice, France, p. 1046(1990)

[8] O. Henry, O. Napoly, Particle Accelerators, 1991, Vol. 35 p. 235

[9] K. L. F. Bane, SLAC-AP-87, June 1991

[10] A. Piwinski, DESY HERA 92-04, January 1992

[11] A. Piwinski, DESY HERA 92-11, May 1992

[12] R. L. Gluckstern, J. van Zeijts, B. Zotter, CERN SL/AP 92-18(1992)

[13] K. Yokoya, KEK Preprint 92-196(1993)

[14] P. Moon and D. E. Spencer: "Field Theory Handbook", 1961

[15] I. S. Gradshteyn and I. Ryzhik: "Tables of Integrals, Series, and Products", 1972

[16] M. Abramowitz and I. A. Stegun: "Handbook of Mathematical Functions", 1984

Appendix A1: Numerical Evaluation

With [15]

$$\int_0^\pi \cos^{2\ell}u\cos(2ku)\,du = \begin{cases} \dfrac{\pi\,(2\ell)!}{4^\ell(\ell-k)!(\ell+k)!} & \text{for } \ell \geq k \\ 0 & \text{for } \ell < k \end{cases} \tag{A1.1}$$

the integral in Eq.(37) can be represented by an infinite sum

$$\begin{aligned} \int_0^\pi \frac{\cos(2k\phi)\,d\phi}{\sqrt{\cosh^2\eta_1-\cos^2\phi}} &= \sum_{\ell=0}^{\infty} \frac{(2\ell)!}{4^\ell(\ell!)^2\cosh^{2\ell+1}\eta_1} \int_0^\pi \cos(2k\phi)\cos^{2\ell}\phi\,d\phi \\ &= \pi\sum_{\ell=k}^{\infty} \frac{((2\ell)!)^2}{2^{4\ell}(\ell!)^2(\ell+k)!\,(\ell-k)!\cosh^{2\ell+1}\eta_1} \end{aligned} \tag{A1.2}$$

$H = H(\eta,\eta_o,\psi,\psi_o)$ can then be calculated by one of the series expansion

$$\begin{aligned} H &= \frac{b}{a}\sum_{n=0}^{\infty}\sum_{m=0}^{\infty}(1+(-1)^{m+n})\Big(\sum_{\ell=(m+n)/2}^{\infty} V_{\ell,(n+m)/2}(A_{n,m}-B_{n,m}) \\ &\qquad + \sum_{\ell=|m-n|/2}^{\infty} V_{\ell,|n-m|/2}(A_{n,m}+B_{n,m})\Big) \\ &= \frac{b}{a}\sum_{\ell=0}^{\infty}\Big(\sum_{m=0}^{2\ell}\sum_{n=0}^{2\ell-m}(1+(-1)^{m+n})V_{\ell,(n+m)/2}(A_{n,m}-B_{n,m}) \\ &\qquad + \sum_{m=0}^{\infty}\sum_{n=m-2\ell\geq 0}^{m+2\ell}(1+(-1)^{m+n})V_{\ell,|n-m|/2}(A_{n,m}+B_{n,m})\Big) \\ &= \frac{b}{a}\sum_{\ell=0}^{\infty}\sum_{k=0}^{\ell}V_{\ell,k}\Big(\sum_{j=0}^{2k}(A_{j,2k-j}-B_{j,2k-j}) \\ &\qquad + (1-\delta_{k,0}/2)\sum_{j=0}^{\infty}(A_{j,2k+j}+B_{j,2k+j}+A_{2k+j,j}+B_{2k+j,j})\Big) \end{aligned} \tag{A1.3}$$

with

$$V_{\ell,k} = \frac{((2\ell)!)^2}{2^{4\ell}(\ell!)^2(\ell+k)!\,(\ell-k)!\cosh^{2\ell}\eta_1}$$

and

$$A_{n,m} = (2-\delta_{o,n})(2-\delta_{o,m})\frac{\cosh(n\eta)\cosh(m\eta_o)}{\cosh(n\eta_1)\cosh(m\eta_1)}\cos(n\psi)\cos(m\psi_o)$$

$$B_{n,m} = 4\,\frac{\sinh(n\eta)\sinh(m\eta_o)}{\sinh(n\eta_1)\sinh(m\eta_1)}\sin(n\psi)\sin(m\psi_o)$$

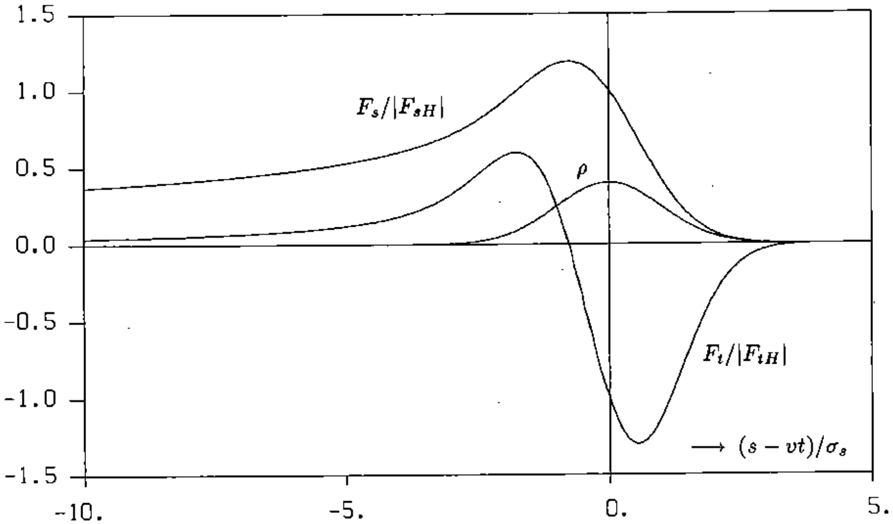

Fig. 1 Longitudinal distribution of the longitudinal (F_s) and transverse (F_t) wakefield forces and of the particle distribution (ρ). $F_{sH} = 2^{3/4} r_e E_o N_p H/(\Gamma(1/4)\, b\, \sigma_s^{3/2} \sqrt{\mu_r Z_o \sigma})$, $F_{tH} = 2^{1/4} r_e E_o N_p (\partial H/\partial y)/(\Gamma(3/4)\, b \sqrt{\mu_r Z_o \sigma \sigma_s})$

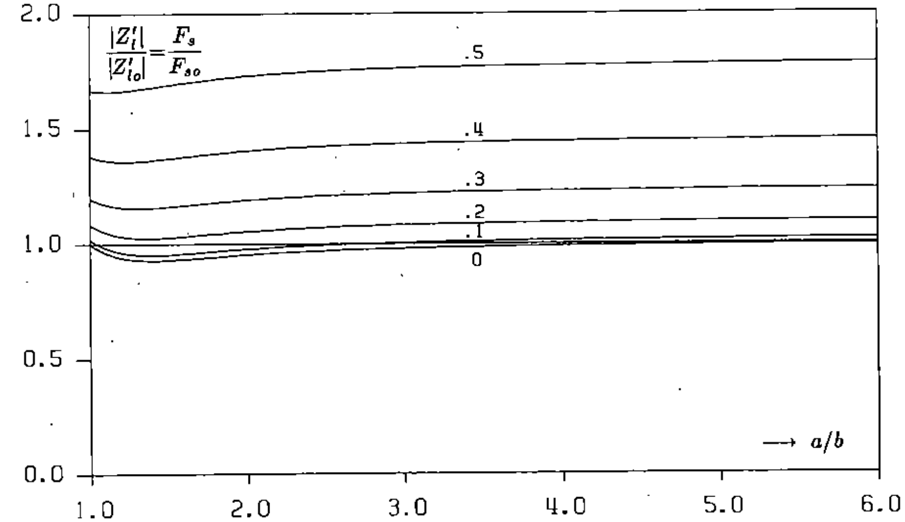

Fig. 2 Dependence of the longitudinal impedance and the longitudinal wake field force on the ratio of the major radius to the minor radius for different vertical positions y_o/b of the beam (x_o=0). $|Z_{\ell o}'| = \sqrt{|\omega|\mu/\sigma}/(2\pi b)$, $F_{so} = 2^{3/4} r_e E_o N_p/(\Gamma(1/4)\, b\, \sigma_s^{3/2} \sqrt{\mu_r Z_o \sigma})$

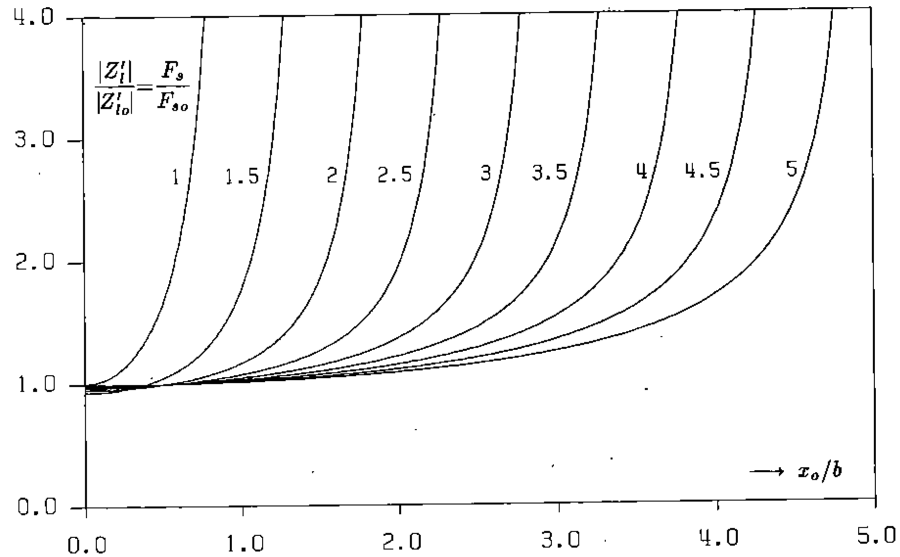

Fig. 3 Dependence of the longitudinal impedance and the longitudinal wakefield force on the horizontal position of the beam for different ratios a/b ($y_o = 0$).

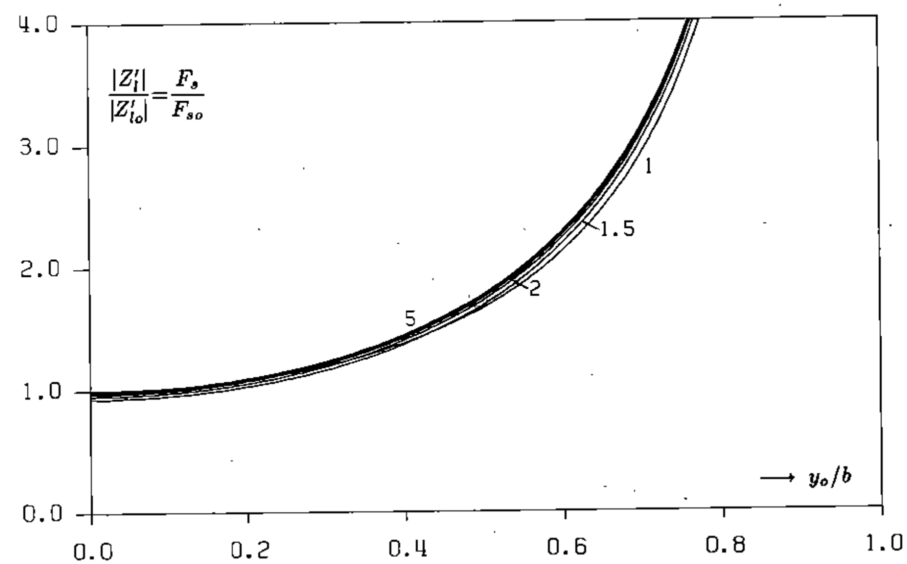

Fig. 4 Dependence of the longitudinal impedance and the longitudinal wakefield force on the vertical position of the beam for different ratios a/b ($x_o = 0$).

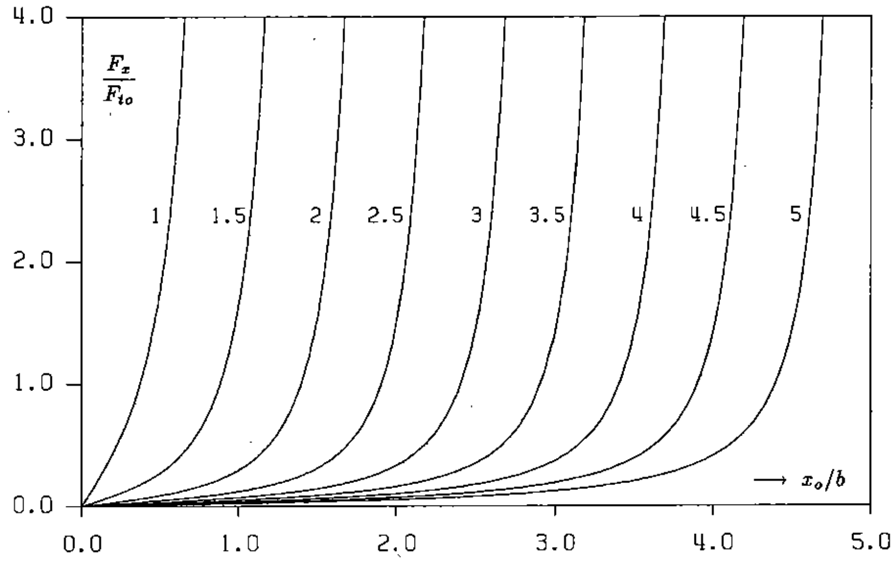

Fig. 5 Dependence of the horizontal wakefield force on the horizontal position of the beam for different ratios a/b (y_o=0). $F_{to} = 2^{1/4} r_e E_o N_p / (\Gamma(3/4) b^2 \sqrt{\mu_r Z_o \sigma \sigma_s})$

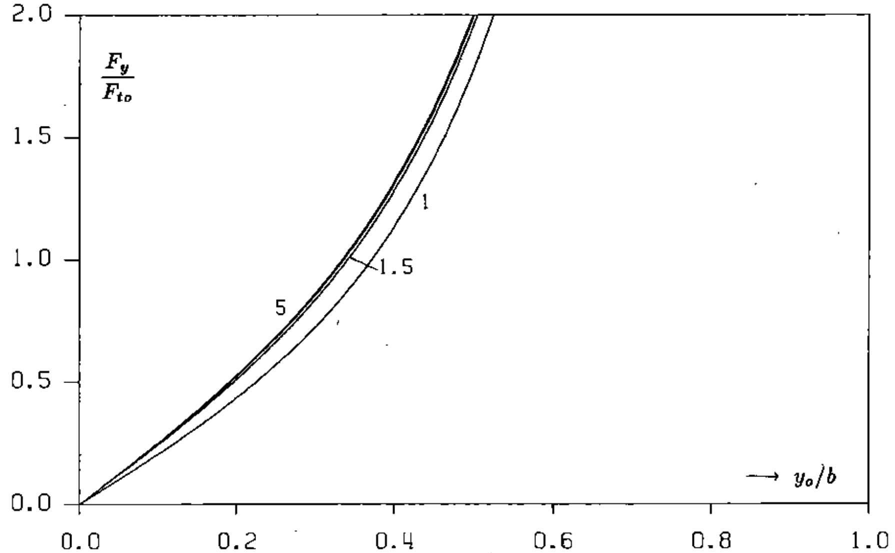

Fig. 6 Dependence of the vertical wakefield force on the vertical position of the beam for different ratios a/b (x_o=0).

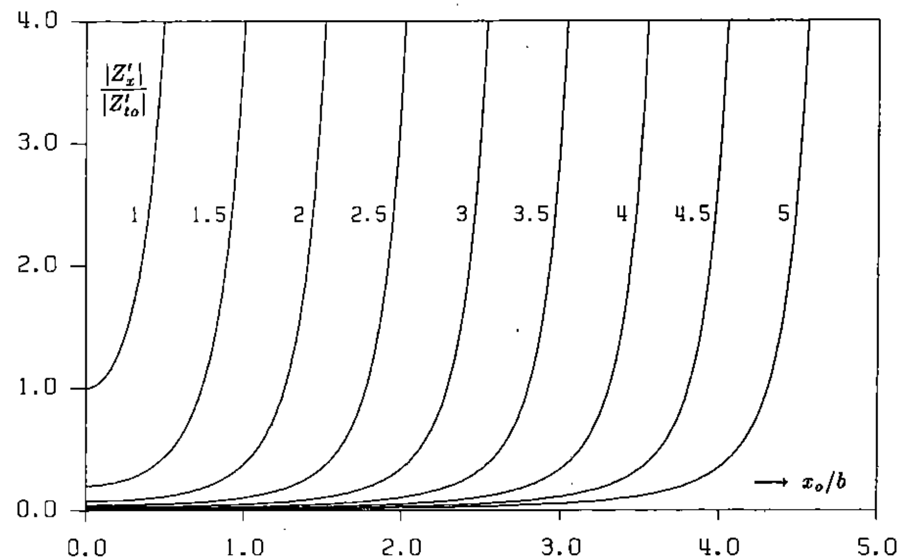

Fig. 7 Dependence of the horizontal impedance on the horizontal position of the beam for different ratios a/b (y_o=0). $|Z'_{to}| = 1/(\pi b^3 \sqrt{|\omega| \epsilon_o \sigma})$

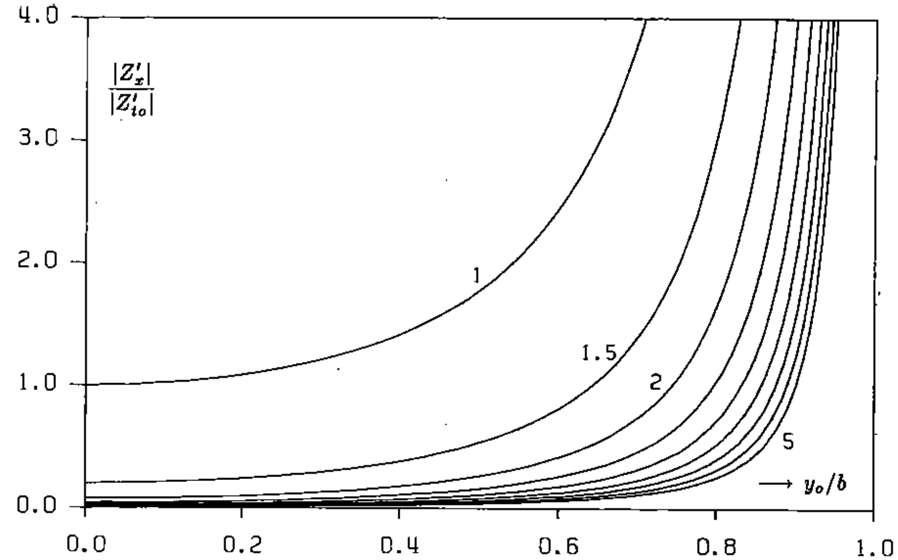

Fig. 8 Dependence of the horizontal impedance on the vertical position of the beam for different ratios a/b (x_o=0).

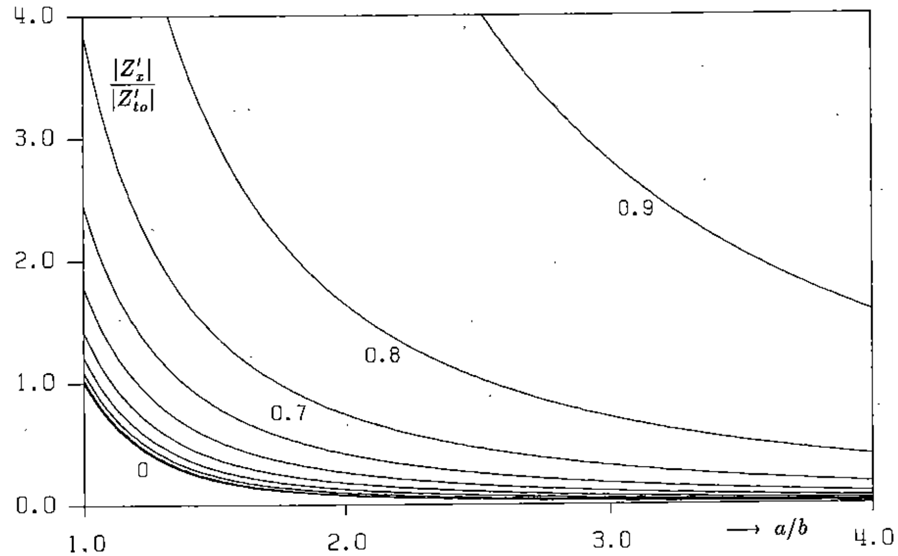

Fig. 9 Dependence of the horizontal impedance on the ratio of the major radius to the minor radius for different vertical positions y_o/b of the beam (x_o=0).

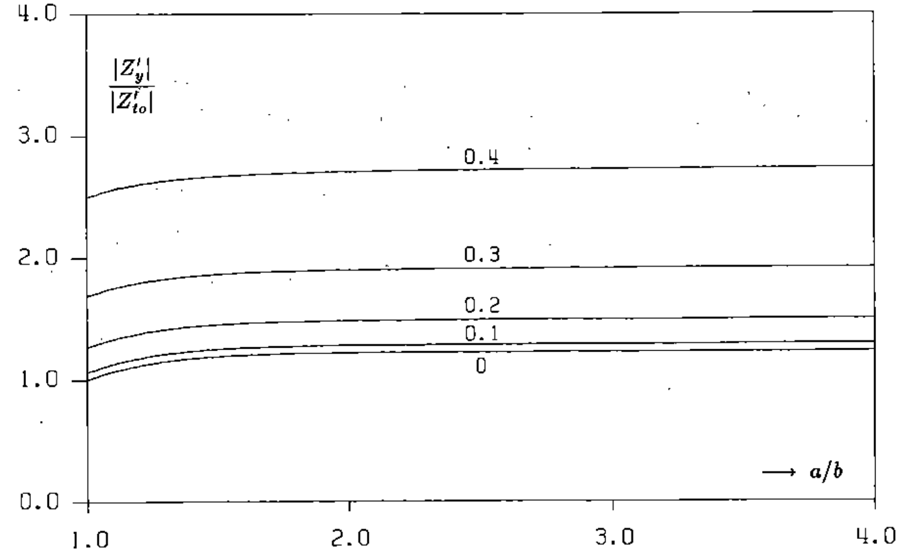

Fig. 10 Dependence of the vertical impedance on the ratio of the major radius to the minor radius for different vertical positions y_o/b of the beam (x_o=0).

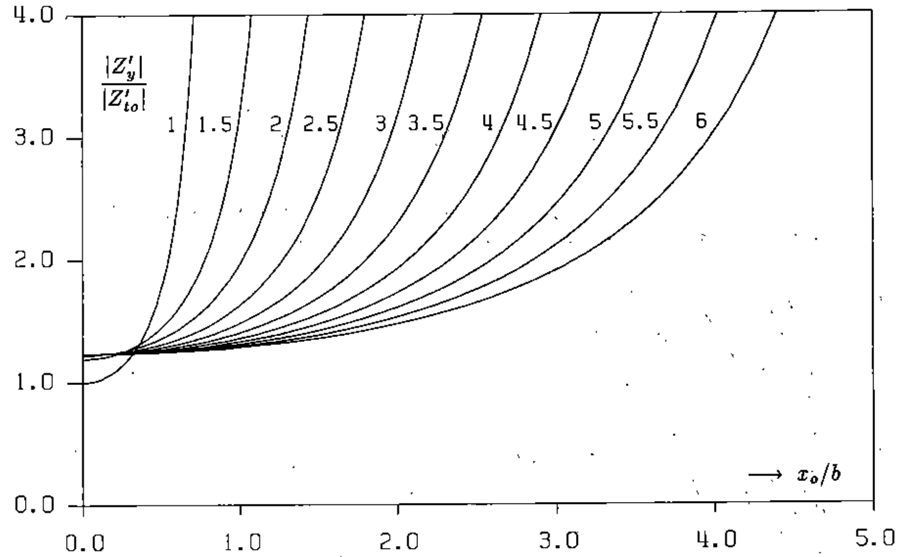

Fig. 11 Dependence of the vertical impedance on the horizontal position of the beam for different ratios a/b (y_o=0). $|Z'_{to}| = 1/(\pi b^3 \sqrt{|\omega|\epsilon_o \sigma})$

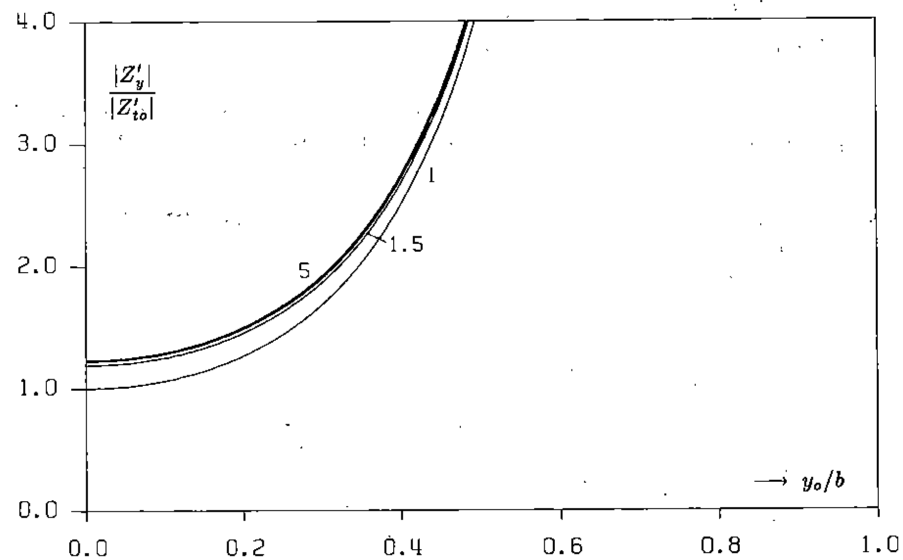

Fig. 12 Dependence of the vertical impedance on the vertical position of the beam for different ratios a/b (x_o=0).